Available online at www.sciencedirect.com
ScienceDirect
Ceramics International 37 (2011) 1833–1837
CERAMICS INTERNATIONAL
www.elsevier.com/locate/ceramint

A comparative study on the magnetic properties of $MFe_{12}O_{19}$ and $MAlFe_{11}O_{19}$ (M = Sr, Ba and Pb) hexaferrites with different morphologies

Sonal Singhal [a,*], Tsering Namgyal [a], Jagdish Singh [b], Kailash Chandra [c], Sandeep Bansal [d]

[a] Department of Chemistry, Panjab University, Chandigarh-160 014, India
[b] Institute Instrumentation Centre, Indian Institute of Technology-Roorkee, India
[c] 33/1, Bhagirath Kunj, Railway Station Road, Roorkee-247 667, India
[d] Department of Metallurgical and Materials Engg., Indian Institute of Technology-Roorkee, India

Received 12 January 2011; received in revised form 3 February 2011; accepted 3 February 2011
Available online 15 February 2011

Abstract

M-type nano hexaferrites $MFe_{12}O_{19}$ and $MAlFe_{11}O_{19}$ (M = Sr, Ba and Pb) have been prepared by the sol–gel method to investigate the shielding effect of inorganic ions KCl, KBr and KI on the phase growth of ferrites. FTIR frequency bands in the range 560–580 cm^{-1} and 430–470 cm^{-1}corresponds to the formation of tetrahedral and octahedral clusters of metal oxides in ferrites, respectively. X-ray powder diffractographs do not show any peaks for the as obtained samples showing the amorphous nature of the samples, however regular peaks for M-type structure have been obtained for all the annealed samples. There is negligible small change in the lattice parameters '*a*' and '*c*' with substitution of the hexagonal ferrites with aluminium. Magnetic measurements showed that the coercivity (Hc) values of all the samples with KCl and KBr enhance due to KCl and KBr to act as deactivators. However, the coercivity value decreases with KI as it oxidise to I_2 during annealing. The saturation magnetization of the hexaferrites decreases with Al^{3+} ion substitution for Fe^{3+} ion due to preferential occupancy of aluminium in octahedral sites.

Keywords: C. Magnetic properties; Hexagonal ferrites; X-ray diffraction and scanning electron microscopy

1. Introduction

Hexagonal ferrite is a class of ceramic magnets having large technological applications as permanent magnets, nanoelectromagnetic devices, microwave devices and magnetic recording media [1]. Garcia-Cerda et al. [2] have synthesized strontium ferrite by sol–gel route and found that the coercivity of the powder increases with increasing temperature up to 800 °C then it decreases with further increase of temperature because of increasing particle size.

Effects of various metal cation substituents on the properties of ferrites are often studied due to their resulting modified properties. A cation distribution mechanism and the doping effect on the magnetic properties of strontium hexaferrites have been investigated by Sandiumenge et al. [3] by synthesizing $SrAl_xFe_{12-x}O_{19}$ $(0 \leq x \leq 12)$ nanoferrites and a decreasing behavior of saturation magnetization with increasing Al^{3+} ion concentration has been observed. However Liu et al. [4] have observed an increasing trend of saturation magnetization with aluminium doping in barium hexaferrite because of weakening of super-exchange interaction between the sub-lattices of Fe^{3+} which leads to anti-parallel alignment of the magnetic moments. Bashkirov and Kostyushko [5] have found that the rate of formation of $SrFe_{9.5}Al_{2.5}O_{19}$ is faster than that of $BaFe_{9.5}Al_{2.5}O_{19}$ because of the higher mobility of Sr^{2+} ions as compared to Ba^{2+} ions. Albanese et al. [6] have synthesized $PbFe_{12-x}Ga_xO_{19}$ hexaferrites and observed that all the samples with $x > 9$ are paramagnetic and further the saturation magnetization decreases with increasing Ga content.

Many attempts have been developed to modify the properties of ferrites among which one is to use inorganic ions because of their ability for selective growth of the samples in particular direction. Yongfei et al. [7] have used inorganic agents like KCl, KBr and KI and reported that the morphology of strontium ferrite is different with all the three cases and coercivity values increases with KCl and KBr while it decreases

* Corresponding author. Tel.: +91 172 2534421; mobile: +91 09872118810.
E-mail address: sonal1174@gmail.com (S. Singhal).

0272-8842/$36.00
doi:10.1016/j.ceramint.2011.02.001

with KI. Well developed hexagonal platelets of $SrFe_{12}O_{19}$ hexaferrites were obtained when it was synthesized by molten salt method using NaCl and KCl [8].

This paper reports the effects of inorganic ions Cl^-, Br^- and I^- on the morphology of $MFe_{12}O_{19}$ and $MAlFe_{11}O_{19}$ (M = Sr, Ba and Pb) hexaferrites. A comparative study of the magnetic properties of the samples with change in morphology has been investigated.

2. Experimental

2.1. Physical measurements

The infrared spectra were recorded using FTIR instrument (PerkinElmer) for all the samples with KBr pellets between the range 4000 and 400 cm^{-1}. The X-ray diffraction studies were carried X-ray diffractometer (Bruker AXS, D8 Advance) with CuKα radiation. SEM characterization was done using LEO (435 VP) instrument. The magnetic measurements were made on a vibrating sample magnetometer (VSM) (155, PAR).

2.2. Preparation of $MFe_{12}O_{19}$ and $MAlFe_{11}O_{19}$ hexaferrrites

$MFe_{12}O_{19}$ and $MAlFe_{11}O_{19}$ (M = Sr, Ba and Pb) hexaferrites at nanoscale have been prepared using sol–gel process [9]. In this method, the desired proportion of precursor nitrates have been separately dissolved in minimum amount of distilled water and heated at 80–90 °C. All the solutions have been mixed and stirred on a magnetic stirrer for sometimes until the nitrates were completely dissolved. Citric acid (in the molar ratio 1:1 to metal nitrates) has been added followed by ethylene glycol to the nitrates solution. The solution has been stirred until gel formation then these gels have been self ignited to obtained $MFe_{12}O_{19}$ and $MAlFe_{11}O_{19}$ (M = Sr, Ba and Pb) hexaferrite powder has been obtained. This hexaferrite powder is mixed with the inorganic agents KCl, KBr and KI separately in the mass ratio 1:3 and annealed at 1000 °C for 2 h to investigate the shielding effect of these ions.

3. Results and discussions

3.1. FT-IR

In the FT-IR spectra of all the ferrites annealed at 1000 °C, the frequency bands in the range 550–580 cm^{-1} and 430–470 cm^{-1} correspond to the formation of tetrahedral and octahedral clusters, which confirms the presence of M–O stretching band in ferrites [10,11]. The authors suggested that the vibrational mode of tetrahedral clusters is higher as compared to that of octahedral clusters, which is due to the shorter bond length of tetrahedral clusters. No peaks have been observed corresponding to the citric acid ($C_6H_8O_7$), which confirms the complete combustion of citric acid. As nujol has

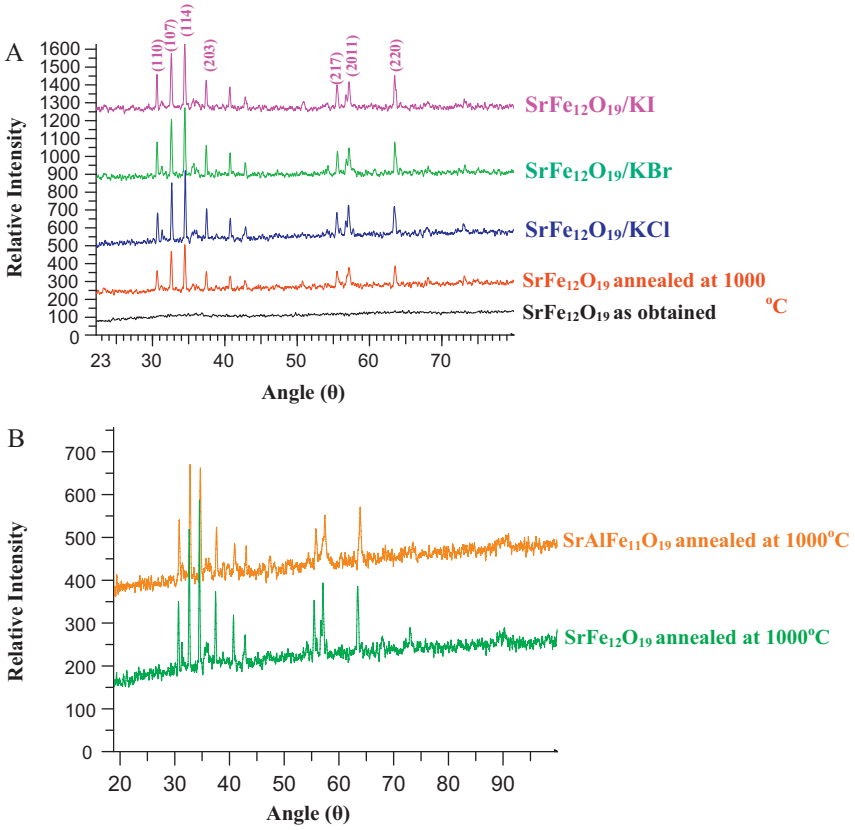

Fig. 1. Powder X-ray diffractographs of (A) $SrFe_{12}O_{19}$ as obtained and annealed at 1000 °C with different inorganic templates and (B) $SrFe_{12}O_{19}$ and $SrAlFe_{11}O_{19}$ after annealing at 1000 °C.

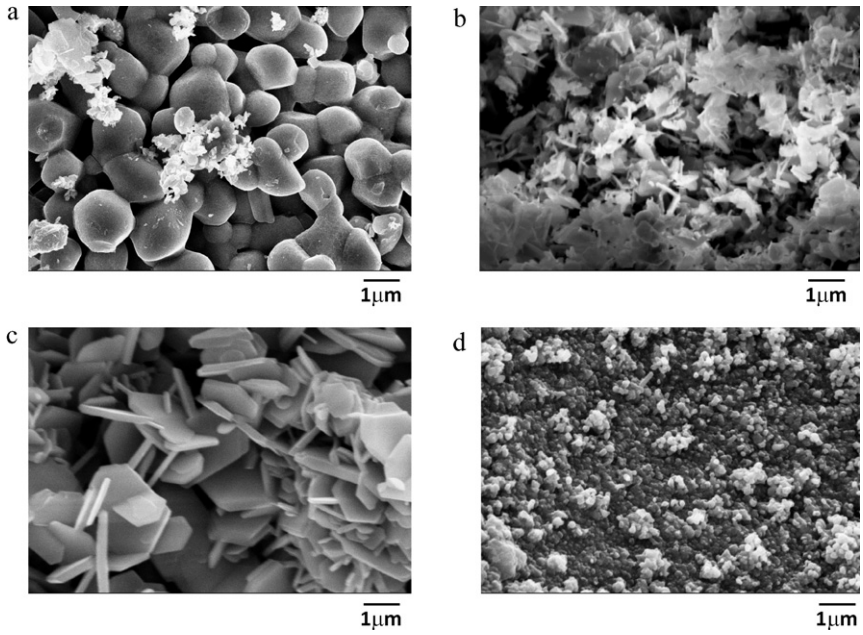

Fig. 2. SEM micrographs of $BaFe_{12}O_{19}$ hexaferrites annealed at 1000 °C with (a) blank, (b) KCl, (c) KBr and (d) KI.

been used as the mulling reagent for the ferrite samples, the frequency bands in the range 3030–2860 cm^{-1}, 1470–1374 cm^{-1} and 719–722 cm^{-1} is attributed to the interference of stretching and bending vibrations of nujol peaks [12].

3.2. X-ray diffraction studies

Typical X-ray diffraction pattern for $SrFe_{12}O_{19}$, as obtained and after annealing at 1000 °C with different inorganic templates are shown in Fig. 1(A). The X-ray diffractographs of all the annealed samples at 1000 °C does not show any peaks corresponding to spinel-type MFe_2O_4 (M = Sr, Ba and Pb) and Fe_2O_3 phases. Therefore it is confirmed that a single phased M-type hexaferrite nanoparticles have been formed in all the cases. It is clear from Fig. 1(A), that the diffraction patterns do not show any peaks for the as prepared ferrite samples thereby showing the amorphous nature of the samples. However the diffraction pattern shows regular peaks for all the annealed samples at 1000 °C corresponding to the magnetoplumbite-type structure formation. As the annealed samples have been properly washed with distilled water to remove the incorporated inorganic ions, so no peaks corresponding to KCl, KBr and KI have been observed in the X-ray diffractographs.

It has been observed that the XRD peaks grew sharper with the addition of inorganic ions in the case of $BaFe_{12}O_{19}$ and $SrFe_{12}O_{19}$, indicating an increase in the particle size [13]. Interestingly, however $PbFe_{12}O_{19}$ being isomorphous with $SrFe_{12}O_{19}$ and $BaFe_{12}O_{19}$ hexaferrites and should give similar results, but the XRD peaks were not sharp when $PbFe_{12}O_{19}$ and $PbAlFe_{11}O_{19}$ were incorporated with the inorganic ions KCl, KBr and KI and this broadening is maximum with KI. Typical X-ray diffractographs of $SrFe_{12}O_{19}$ and $SrAlFe_{11}O_{19}$ are shown

Table 1
Coercivity and saturation magnetization values of $MFe_{12}O_{19}$ and $MAlFe_{11}O_{19}$ (M = Sr, Ba and Pb) hexaferrites annealed at 1000 °C.

(M=)	Inorganic ion used	$MFe_{12}O_{19}$		$MAlFe_{11}O_{19}$	
		Coercivity[a] (Oe)	Saturation magnetization[b] (emu/g)	Coercivity[a] (Oe)	Saturation magnetization[b] (emu/g)
Sr	Blank	4897	54.33	5950	23.82
	KCl	6125	30.41	7075	31.70
	KBr	5780	42.45	6075	29.63
	KI	5400	48.25	6025	36.08
Ba	Blank	4975	50.35	2059	20.82
	KCl	5025	52.36	3237	9.47
	KBr	4850	56.40	2950	16.73
	KI	3600	52.32	700	24.32
Pb	Blank	2420	46.44	2775	37.05
	KCl	3780	35.97	5500	15.59
	KBr	3570	3.40	5220	17.60
	KI	950	0.06	1325	10.52

[a] Coercivity has uncertainty ± 10 Oe.
[b] Saturation magnetization has uncertainty ± 0.02 emu/g.

in Fig. 1(B) to observe the effect of Al^{3+} ion substitution for Fe^{3+} ion. M-type structure has also been observed for the aluminium substituted hexaferrites with and without the inorganic ions however the peaks shifted to negligibly lower angles. The lattice parameters '*a*' and '*c*' have been calculated using Powley and Le-Bail refinement methods and it has been observed that the lattice parameters of $MAlFe_{11}O_{19}$ (M = Sr, Ba and Pb) hexaferrites are negligibly smaller than those of $MFe_{12}O_{19}$ (M = Sr, Ba and Pb) hexaferrites attributing to the small amount of Al^{3+} ion (53.5 pm) substitution with Fe^{3+} ion (64.5 pm).

3.3. SEM characterization

Fig. 2 shows typical SEM images of $BaFe_{12}O_{19}$, $BaFe_{12}O_{19}$/KCl, $BaFe_{12}O_{19}$/KBr and $BaFe_{12}O_{19}$/KI samples annealed at 1000 °C. Fig. 2(a) shows the agglomerated rounded morphology of the sample without any inorganic ion. When the nanoferrite samples have been incorporated with the inorganic ions (KCl, KBr and KI), the morphology of the nanoferrite samples gets modified according to the shielding ability of the ions. Fig. 2(b) and (c) shows that the agglomerated sample shielded along a crystal axis and thin hexagonal platelets have been obtained with KCl and KBr. It means that the morphology anisotropy of the samples gets increased with incorporation of KCl and KBr. The platelets have different thickness depending on the ability of the ions to deactivate various phases of hexaferrites. The greater thickness of the platelets with KBr as compared to KCl shows that KBr has lesser tendency of allowing the sample to grow in a particular direction. However with KI the hexagonal platelets were absent and a less agglomerated spherical shape of the sample has been observed which shows the inability of KI to act as deactivating agent [Fig. 2(d)]. Hence morphology of the sample can be easily tuned according to the research interest by incorporating with inorganic template agent.

3.4. Magnetic measurements

Hysteresis loop for all the samples have been recorded at room temperature and the data obtained from the hysterisis loops are given in Table 1. Typical hysteresis loops of $SrFe_{12}O_{19}$/Blank, $SrFe_{12}O_{19}$/KCl, $SrFe_{12}O_{19}$/KBr and $SrFe_{12}O_{19}$/KI hexaferrites after annealed at 1000 °C are shown in Fig. 3(A) to observe the effect of these inorganic agents. From Table 1, it has been observed that the coercivity of all the ferrites with KCl and KBr gets enhanced whereas it gets decreased when it was annealed with KI. This change in coercivity is due to the reason that the morphology anisotropy increases with KCl and KBr having ability to shield the phases and growth of hexaferrites in a particular direction whereas KI with annealing gets oxidized to I_2 and I^- and is unable to act as shielding agent [7]. The anions Cl^- and Br^- with high coordination ability is absorbed to the crystal face of $SrFe_{12}O_{19}$ micro-crystal to take the shielding effect. These anions will influence the crystal face shielded and will have little effect on other crystal faces, making the growth rate of different crystal faces different [14]. The increase of morphology anisotropy with KCl and KBr has also been confirmed with the SEM results. The saturation magnetization for $SrFe_{12}O_{19}$/KI is 54.33 emu/g compared to that of $SrFe_{12}O_{19}$/Blank is 48.25 emu/g and this trend of increase of saturation magnetization with KI is same for the samples $MFe_{12}O_{19}$ and $MAlFe_{11}O_{19}$ (M = Sr and Ba). Typical hysteresis loops of $PbAlFe_{11}O_{19}$/Blank, $PbAlFe_{11}O_{19}$/KCl, $PbAlFe_{11}O_{19}$/KBr and $PbAlFe_{11}O_{19}$/KI hexafer-

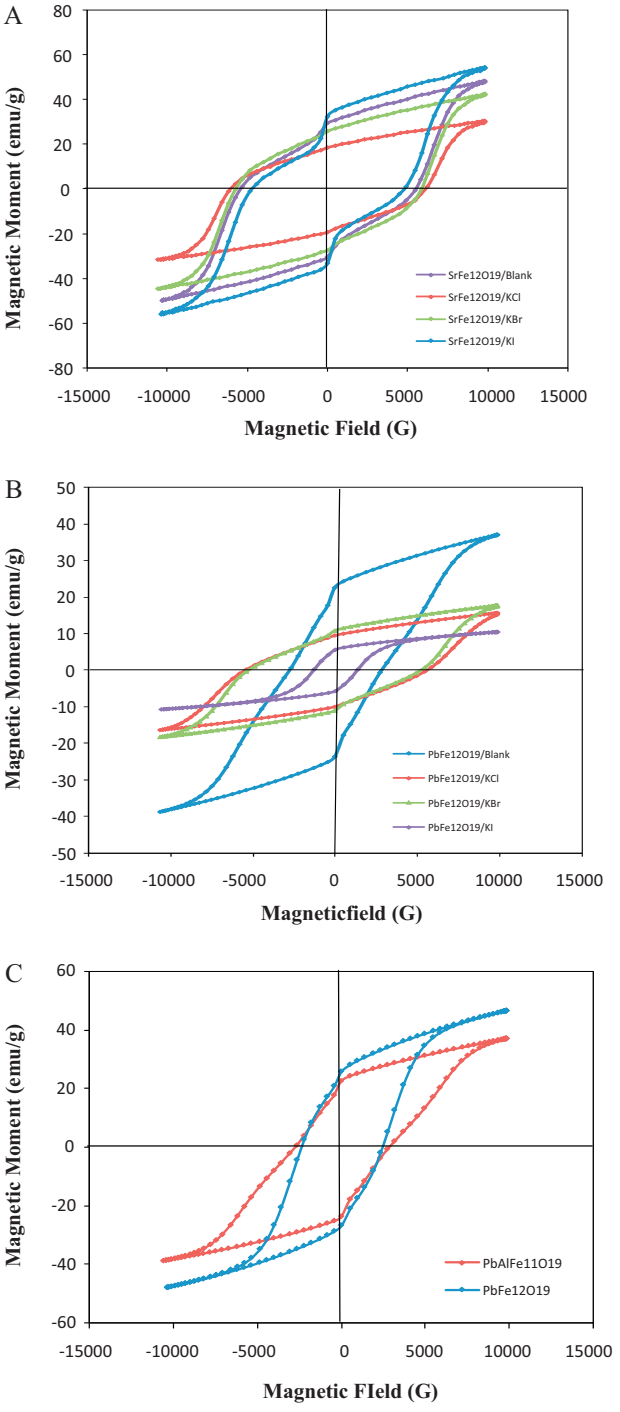

Fig. 3. Hysteresis loops of (A) $SrFe_{12}O_{19}$ hexaferrites annealed at 1000 °C with different morphologies, (B) $PbAlFe_{12}O_{19}$ hexaferrites annealed at 1000 °C with different morphologies and (C) $PbFe_{12}O_{19}$ and $PbAlFe_{11}O_{19}$ hexaferrites annealed at 1000 °C.

rites after annealed at 1000 °C are shown in Fig. 3(B). It is clear from this figure that, for $PbFe_{12}O_{19}$ and $PbAlFe_{11}O_{19}$ with KI, the saturation magnetization values decreases attributing to a decrease in the particle size which is already discussed in X-ray diffraction studies.

Fig. 3(C) shows the typical hysterisis loop of $PbFe_{12}O_{19}$ to see the effect of aluminium substitution on the magnetic properties of ferrites. It has been observed that the saturation magnetization decrease with Al^{3+} ion substitution. In $MFe_{12}O_{19}$ (M = Sr, Ba and Pb) there are five non equivalent sublattices of which three are octahedral (2a, 12k and $4f_2$), one tetrahedral ($4f_1$) and one trigonal bipyramidal (2b) [15]. Further it has been found that whereas 12k, 2a and 2b have their spins in upward direction, $4f_1$ and $4f_2$ have downward spin and the resulting magnetic moment of $MFe_{12}O_{19}$ (M = Sr, Ba and Pb) is due to the upward spins. Now when Al^{3+} ions (diamagnetic) are substituted for Fe^{3+} ions, this decrease in M_s value is because of decrease of the superexchange interaction ($Fe_A{}^{3+}$–O–$Fe_B{}^{3+}$) as the Al^{3+} ions preferencially occupies the octahedral 2a sites followed by 12k and $4f_2$ sites [16]. There is also an increase in coercivity value with this substitution which may be due to increase in magnetic anisotropy [17].

4. Conclusion

$MFe_{12}O_{19}$ and $MAlFe_{11}O_{19}$ (M = Sr, Ba and Pb) hexaferrite powder has been successfully prepared by sol–gel method. The formation of the hexagonal ferrites was confirmed by FT-IR spectroscopy and X-ray powder diffraction studies. FT-IR spectra showed the formation of the corresponding M–O stretching bands in ferrites. X-ray powder studies indicate a single phased M-type structure for all the hexaferrite samples. The lattice parameters of substituted hexaferrites were negligibly smaller than those of undoped ones. SEM results showed that the morphology of the samples was successfully changed by adding different inorganic template agents like KCl, KBr and KI. The morphology anisotropy was increased with KCl and KBr hence an enhanced coercivity values were observed in these cases. However with KI the coercivity value was not improved because morphology anisotropy was not increased with KI as it gets oxidized to I_2. The saturation magnetization decreases with Al^{3+} ion doping in $MFe_{12}O_{19}$ (M = Sr, Ba and Pb) hexaferrites due to the diamagnetic nature of Al^{3+} ion.

Acknowledgement

Grateful thanks to the UGC for the financial support for this research work under the scheme of UGC-major project.

References

[1] I.V. Zavislyak, M.A. Popov, G. Srinivasan, Meas. Sci. Technol. 20 (2009) 115704–115708.
[2] L.A. Garcia-Cerda, O.S. Rodriguez-Fernandez, P.J. Resendiz-Hernandez, J. Alloys Compd. 369 (2004) 182–184.
[3] F. Sandiumenge, S. Gali, J. Rodriguez, Mater. Res. Bull. 23 (1988) 685–692.
[4] Y. Liu, M.G.B. Drew, J. Wang, M. Zhang, Y. Liu, J. Magn, Magn. Mater. 322 (2010) 366–374.
[5] L.A. Bashkirov, Y.L. Kostyushko, Inorg. Mater. 39 (2003) 392–397.
[6] G. Albanese, F. Leccabue, B.E. Watts, S. Diaz-Castanon, J. Mater. Sci. 37 (2007) 3759–3763.
[7] W. Yongfei, L. Qiaoling, Z. Cunrui, J. Hongxia, J. Alloys Compd. 467 (2009) 284–287.
[8] S. Kim, J. Kim, J. Magn, Magn. Mater. 307 (2007) 295–300.
[9] S. Singhal, T. Namgyal, S. Bansal, K. Chandra, J. Electromagn. Anal. Appl. 2 (2010) 376–381.
[10] A. Pradeep, G. Chandrasekaran, Mater. Lett. 60 (2006) 371–374.
[11] F.M.M. Pereira, C.A.R. Junior, M.R.P. Santos, R.S.T.M. Sohn, F.N.A. Freire, J.M. Sasaki, J.A.C. De-Paiva, A.S.B. Sombra, J. Mater. Sci.: Mater. Electron. 19 (2008) 627–638.
[12] R.M. Silverstein, F.X. Webster, Spectroscopic Identification of Organic Compounds, 6th ed., Wiley, 2006, pp. 74–143, chapter 3.
[13] H.P. Klug, L.E. Alexender, X-ray Diffraction Procedures for Polycrystalline and Amorphous Materials, 2nd ed., Wiley, 1974, pp. 491–538, chapter 9.
[14] G.H. Li, D.W. Wang, Z.L. Huang, J. Synth. Crystals 16 (2001) 338–339.
[15] L. Lechevallier, J.M.L. Breton, J.F. Wang, I.R. Harris, J. Magn, Magn. Mater. 269 (2004) 192–196.
[16] M.J. Iqbal, M.N. Ashiq, P. Hernandez-Gomez, J.M. Munoz, J. Magn, Magn. Mater. 320 (2008) 881–886.
[17] S. Wang, J. Ding, Y. Shi, Y.J. Chen, J. Magn, Magn. Mater. 219 (2000) 206–212.